Occurrence and source of PAHs in Miankaleh International Wetland in Iran

Mahsa Rokhbar [a], Behnam Keshavarzi [a,*], Farid Moore [a], Mehdi Zarei [a], Peter S. Hooda [b], Michael J.Risk [c]

[a] Department of Earth Sciences, College of Science, Shiraz University, 71454 Shiraz, Iran.

[b] Department of Geography, Geology and the Environment, Kingston University London, Kingston Upon Thames KT12EE, UK.

[C] Department of Earth Sciences, McMaster University, Hamilton, Ontario, L8S 4M1, Canada.

[*] Corresponding author.

E-mail addresses: BKeshavarzi@shirazu.ac.ir (B. Keshavarzi).

Abstract
We examined the occurrence and sources of 16 priority PAHs in the water and sediment samples of the Miankaleh Wetland (Coastal Biosphere Reserve), famous for harbouring huge flocks of migrating birds. The water and sediment samples collected from various locations were visualized and processed using a self-organizing map, positive matrix factorization and GIS. All the sediment samples, and >90% of the water samples, showed some degree of PAHs contamination. Higher PAH levels occur near the Chopoghi Channel, powerplants, sewage outfalls, and near fishing operations. Compared with previous study in this area, the PAHs concentration in the sediments of aquatic ecosystem of Miankaleh Wetland is increasing. The levels of PAH contamination seem too low to account for the mass deaths of migratory birds, and botulinus contamination seems the likely cause. Fugacity calculations show that the sediments act as a sink for PAHs. According to PMF and SOM analyses, three origins of PAHs were recognized: (i) fossil fuel and vehicular emissions with high-molecular weight PAHs (4-5 ring); (ii) municipal and industrial sewages characterized by low-molecular weight PAHs (2-3 ring) typical of petrogenic sources; and (iii) port activity characterized by prevalence of petrogenic influence and petroleum-related activities (combustion PAHs and low-molecular weight PAHs) consistent with port activity. This wetland needs serious attention because of continuous input of pollutants. The results and the methods used in this study may assist in improving coastal wetlands management.
Key words: PAHs, Spatial distribution, Fugacity fraction, Source apportionment, Miankaleh Wetland

Graphical Abstract

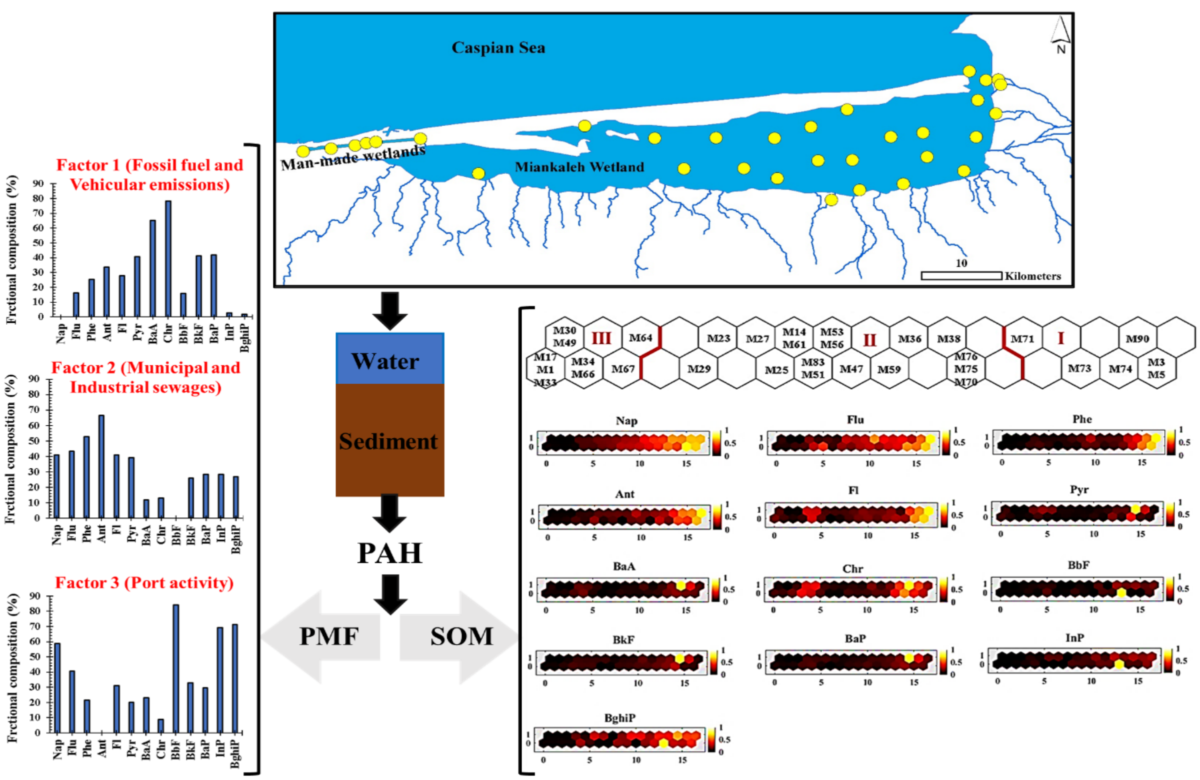

1. Introduction

Polycyclic aromatic hydrocarbons or PAHs are known as environmental contaminants with resistant, toxic and genotoxic characteristics which may induce carcinogenic, mutagenic and toxic effects in human and aquatic biota (Bianco et al., 2020; Jia et al., 2021; Khiari et al., 2021). For this reason, the environmental fate and potential ecological risks of PAHs have attracted global attention (e.g., Chen et al., 2020a). There are numerous PAHs but currently only 16 of them are prioritized as important pollutants by the United State Environmental Protection Agency, USEPA (Gao et al., 2018). PAHs often have strong affinity for sediments in aquatic environment, mostly because of low solubility, poor volatility and high octanol-water partition coefficient (K_{ow}). Consequently, sediment is the most useful archive for documenting and studying these hydrophobic organic pollutants (Du and Jing, 2018). These pollutants are usually classified as low-molecular weight with 2 or 3 benzene rings (LMW) that are normally dominant in water, and high-molecular weight with 4 or 6 benzene rings (HMW) which usually prevail in sediments (Ambade et al., 2021a; Zhao et al., 2021b). However, PAHs may resuspend in sediments and redissolve into the overlying water column, causing secondary pollution under turbulent conditions (Zhao et al., 2021a). The occurrence of PAHs is commonly related to natural and human activities, but the source of PAHs is mostly either pyrogenic (fossil fuel combustion, vehicular emissions, waste incineration, etc.) or/and petrogenic (oil exploitation, industrial wastewater, surface runoff and untreated sewage). Various factors affect the source and amount of PAHs release in the environment; additionally, the effect of lockdown due to covid-19 on the release of PAHs has also been debated in recent literature (Ambade et al., 2021c and d). Hence PAHs are recognized as useful indicators to assess anthropogenic activities and their environmental impacts (Ambade et al., 2021b; Li et al., 2021; Pichler et al., 2021; Zhang et al., 2021).

Wetlands are valuable ecosystems in the biosphere at local and global scales, and recognized as key ecological tools, since many essential ecological functions such as maintaining ecosystem diversity, providing habitat and shelter for unique flora1 and fauna1 species including rare and endemic species, purification of runoff, flood control, conservation of soil against erosion, natural groundwater recharge and climate regulation (Townsend et al., 2019; Mereta et al., 202; Oja et al., 2021). Moreover, wetlands promote human well-being by providing food, energy, increasing tourism potential and cultural impacts (Cui et al., 2018). However, due to human activities wetlands quality has decreased or degraded worldwide (Xu et al., 2019; Jisha and Puthur, 2021), mostly due to a wide range of pressures including eutrophication, aquaculture, groundwater levels depletion, changing land use, soil erosion, inappropriate tourism, deforestation, urbanization, road development and pollution (Cai et al., 2021; Sadeghi Pasvisheh et al., 2021). Since the negative effects of human activity on wetlands are yet to be fully understood (Xiu et al., 2019), it is therefore essential to examine the causes of wetlands degradation. The results can assist in setting up efficient management policies and protection plans (Wang et al., 2022).

Miankaleh International Wetland (Coastal Biosphere Reserve) has been recognized as a “Ramsar site” since 1975 because of its cultural inheritance, historical, biological and esthetic characteristics (Gholami et al., 2020; Alipour et al., 2015). Miankaleh Wetland is a protected region, located on the southeast part of the Caspian Sea (Iran), a rich ecosystem and ecological haven in Asia (Ranjbar Jafarabadi et al., 2020). This wetland is the most significant wintering area for waterbirds in Caspian Sea region (Alipour et al., 2015), which is an internationally recognized sanctuary for migratory birds (Gholami et al., 2020; Sinkakarimi et al., 2018). It is also a significant marine habitat for the sturgeon that the locals around the wetland rely on (Ranjbar et al., 2019). Also, more than half of the Caviar produced in Iran comes from this area (Kheirabadi et al., 2018). This wetland has been in the focus of attention in recent years because of all the sudden death of thousands of migratory birds (World Photography Organisation, 2022).

Miankaleh Wetland, with a west-east trend and an altitude of 15 to 30 m below mean sea level, has a surface area of about 68800 ha and is located southeast of the Caspian Sea (50' 36" N and 53' 45" E; Fig. 1). This wetland has both an aquatic ecosystem of Gorgan Bay (semi enclosed and brackish) with an area of about 44800 ha (Ranjbar Jafarabadi et al., 2020), and a land ecosystem with a relatively narrow strip called Miankaleh Peninsula with an area of about 24000 ha. Miankaleh Peninsula separates the Miankaleh Wetland (with a maximum depth of about 6.5 m and a mean depth of about 1.8 m) from the Caspian Sea (Mansoori, 2009) which increases from west to east, with a clockwise direction of flow. Miankaleh Wetland is linked to the Caspian Sea through Chopoghli channel, and the Caspian Sea supplies water through this channel (Kheirabadi et al., 2018; Kouhanestani et al., 2019). Therefore, the water level of Miankaleh Wetland is directly related to the Caspian Sea (Ranjbar and Hadjizadeh Zaker, 2018) which has dropped in recent years because of the lowering of Caspian Sea water level (Gholizadeh and Patimar, 2018; Isaie Moghaddam et al., 2021). Also, the wetland receives freshwater from precipitation (60 cm/year), man-made wetlands (Zaghmarz Lapoo, Shirkhan Lapoo and Palangan Lapoo) and several small seasonal rivers with Qareh Sou river in the southeast part of the wetland being the main and having the largest freshwater flow into the wetland (Leroy et al., 2019; Gholami et al., 2020; Kousali et al., 2022). In all, 62% of the fresh water entering the Miankaleh Wetland is supplied by this river (flow of 800 L/s) (Ranjbar et al., 2019; Ranjbar and Hadjizadeh Zaker, 2018). The rate of evaporation in this region is about of 124.1 cm/year and the mean annual temperature is 18 °C (warm and semi humid) (Ranjbar et al., 2019; Gholami et al., 2020). This wetland may become most degraded ecosystem in Iran in the foreseeable future as a result of continuous inputs of pollutants and nutrients as seen in recent years (Bagheri et al., 2020; Maleki et al., 2020), mostly from the expansion of agriculture, transport emissions, wastewater from slaughterhouses, fish farming, the Neka Powerplant which uses mazut (heavy and low-quality fuel oil), port activities (e.g., Neka Port, Amirabad Port) and municipal and industrial wastewater discharges. These anthropogenic stresses undoubtedly endanger the food chains and wildlife (Zafarani et al., 2022), resulting in general degradation in water quality due to eutrophication (Kouhanestani et al., 2019).

The positive matrix factorization model (PMF) is an efficient means of recognizing the source apportionment and quantifying the contributions of recognized origins (Zhang et al., 2019). The self-organizing map (SOM) is an artificial neural network and a method of graphical clustering (Lee et al., 2021; Kumar et al., 2021). In this study, we applied PMF model and SOM to examine the sources and distribution of PAHs, which can help with source-oriented reduction strategies. In 2017, PAHs in the sediment from 6 stations of the Gorgan Bay (part of the larger wetland system) were determined by Zafarani et al., (2022). PAH isomeric ratios showed that contamination originated from pyrogenic sources. Furthermore, the results of previous studies proved that due to changes in the physicochemical conditions of water and sediments, favorable conditions have been provided for biotoxin production, and as a result, Clostridium botulinum poisoning has caused the death of more than 35,000 migratory birds (Maken Ali et al., 2020; Parchizadeh and Belant, 2020). Given the limited scope of this previous study, further investigation of water and sediment in Miankaleh Wetland were deemed necessary for establishing the level of PAH contamination. Because lack of management and control of the conditions of this sensitive ecosystem, will lead to repeated bird losses in the coming years. Also based on importance of this wetland in terms of fishing and Caviar, it is important to investigate and monitor the extent, degree and source of pollutants in this wetland. This work is the first comprehensive PAHs investigation in sediments and water of Miankaleh Wetland and is aimed to quantify the effects of anthropogenic activities on PAHs levels, with the following objectives: (i) investigate PAHs concentration and assess their pollution levels in Miankaleh Wetland; (ii) recognize the potential sources and distribution of PAHs using PMF, geographical information system and SOM.

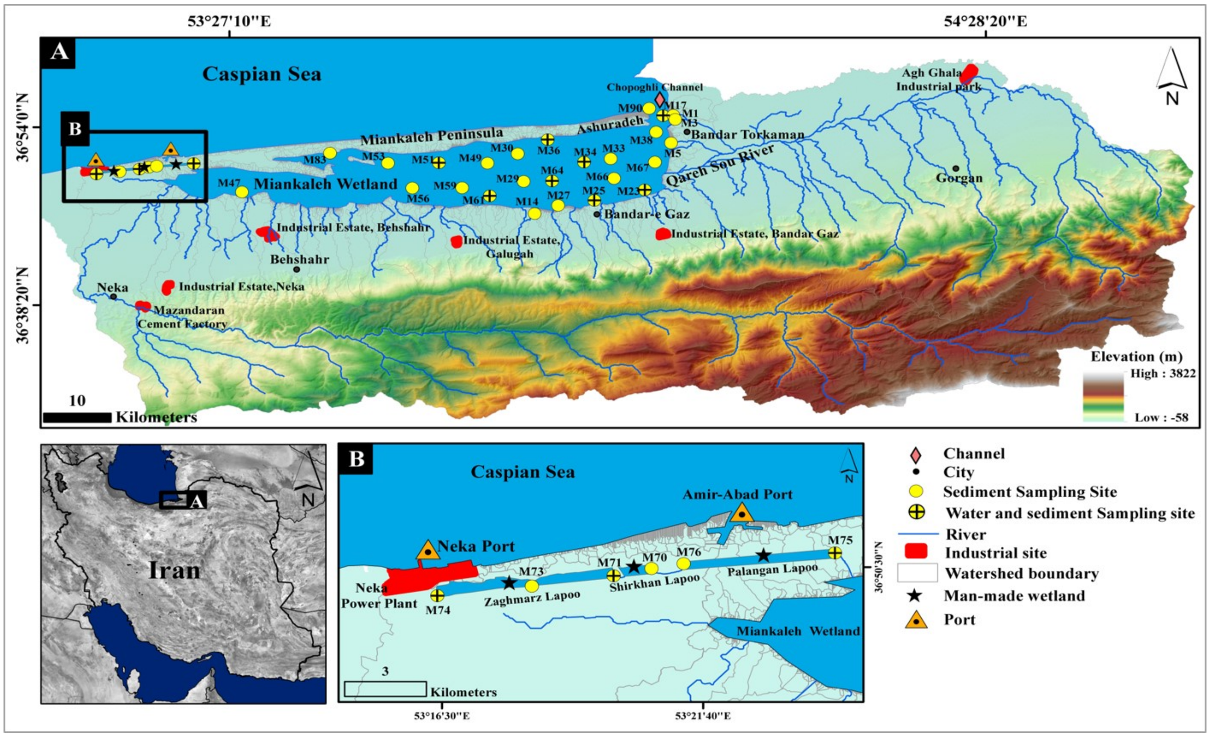

Fig. 1. The study area of the Miankaleh Wetland, showing the sampling sites.

1. Materials and methods

2.1 Sediment-Water Sampling

Sampling was done in the dry season (September 2020). The sampling stations were selected according to previously available information (Bagheri et al., 2020; Ranjbar et al., 2018; Kouhanestani et al., 2019), together with known sources of potential pollution, such as fish farms, agricultural effluents, urban pollution and sewage, and slaughterhouse wastewater inputs in the Miankaleh Wetland. The sampling stations, however, were generally distributed evenly in the area (Fig. 1). Thirty-two sampling stations were selected where surface sediment samples were collected by a stainless-steel Van-Veen grab (0-10 cm in depth); each sample was comprised of four homogenized individual subsamples, within an area of 6 m^2 at each sampling location. GPS positioning (GPS Gerät-Etrex 10 Worldwide) was used to determine the location of sampling stations. Before sampling, the sediment sampler was washed thrice with water from the sampling site. All sediment samples were straightaway transferred to amber glass jars pre-cleaned using distilled water and n-Hexane (Abbasi et al., 2019; Sheikh Fakhradini et al., 2019) before being completely sealed with gas-tight aluminum caps. All Samples were stored in iceboxes (<4 °C) and carried to the laboratory. In the laboratory, the samples were placed at −20 ºC before their analysis, within a month after their collection. Of the 32 sampling stations, 11 were randomly chosen for water sampling as water PAHs usually are less variable compared to their levels in sediments (Sheikh Fakhradini et al., 2019). At each of these 11 stations (from the water column above the sediment), 2 L of water sample in triplicate was collected using amber glass bottles pre-cleaned using distilled water and n-Hexane, before storing at 4 °C, and pretreating the samples within 24 h.

2.2 Physicochemical parameters

Main physicochemical parameters of the water samples, such as pH, temperature, electrical conductivity (EC), redox potential (Eh) and dissolved oxygen (DO) were assessed in situ via a multi parametric (CyberScan PCD 650 Eutech) portable instrument. The results are briefed in Table S1 (Supplementary Information). Sediments subsamples were sieved through a 2 mm sieve after drying at <30°C (room temperature), which were used to determine their physicochemical characteristics including grain size, calcium carbonate content ($CaCO_3$), organic matter (OM), pH, cation exchange capacity (CEC), EC and distribution of particle size using standard protocols, and the results are summarized in Table S2 (Supplementary Information). The organic matter (OM) content in the sediment samples was determined based on loss-on-ignition (LOI) at 500 °C for 4 h (Frena et al., 2016). The calcium carbonate content was determined by LOI at 950 °C for 2 h (Tenkouano et al., 2019).

Table 1. PAHs concentrations in the water of Miankaleh Wetland and specified concentration thresholds (maximum concentrations)

unit: ng/L	P value [a]	LOD	Min[b]	Max.[c]	Mean[d]	Med.[e]	S.D.[f]	C.V.[g]	(US EPA)	European Union	Canada (fresh water)	Canada (Marin water)
Nap	0.00	1.20	1.75	512.00	99.52	49.88	138.97	1.40	_	2.40×10^3	1.10×10^3	1.40×10^3
Flu	0.00	0.50	0.38	12.21	4.57	3.91	4.02	0.88	2.00×10^4	100.00	40.00	_
Phe	0.20	0.80	0.60	25.55	8.81	9.26	7.88	0.89	_	_	400.00	_
Ant	0.10	0.50	0.38	11.40	4.42	3.96	3.94	0.89	4.00×10^5	100.00	12.00	_
Fl	0.10	0.50	0.38	7.81	3.24	2.79	2.18	0.67	7.00×10^4	_	3.00×10^3	_
Pyr	0.60	0.50	1.51	12.23	6.09	6.99	2.90	0.48	3.00×10^4	_	25.00	_
Chr	0.00	0.60	0.45	2.96	1.23	0.82	0.91	0.74	130.00	_	_	_
∑PAHs			10.61	564.28	127.87	71.96	148.23	1.16	_	_	_	_
∑ 2-3 rings			3.35	546.96	117.32	57.48	146.13	1.25				
∑ 4-6 rings			4.17	18.68	10.56	10.81	4.63	0.44				
LMW/HMW			0.46	33.42	11.86	7.88	11.48	0.97				

[a] P value calculated by Shapiro-Wilk test
[b] Min.: the minimum value
[c] Max.: the maximum value
[d] Mean: the arithmetic average
[e] Med.: Median value
[f] S.D.: the standard deviation value
[g] C.V.: Coefficient of variation value

2.3 PAHs assessment

For extracting PAHs from sediment and water samples, two standard methods EPA3550B and EPA3510C were used respectively. Prior to the analysis following EPA guideline 8310, a cleanup method EPA3630C was used. For analytes, a LiChrospher© PAH column (250 mm, 4.6 mm, 5 µm) was used. The 20 µL subsample aliquots were injected by syringes. The mobile phase was formed consisting of Acetonitrile and water at 35°C temperature in a gradient mode and 1 mL/min flow rate. Analyses of 16 target PAHs in the samples including Anthracene (Ant), Acenaphthene (Ace), Benz[a]anthracene (BaA), Benz[a]pyrene (BaP), Benz[b]fluoranthene (BbF), Acenaphthylene (Acy), Benz[ghi]perylene (BghiP), Benz[k]fluoranthene (BkF), Fluorene (Flo), Indeno[1,2,3 cd]pyrene (InP), Chrysene (Ch), Dibenz[a,h]anthracene (DahA), Naphthalene (Nap), Fluoranthene (Flu), Phenanthrene (Phe), and Pyrene (Pyr) were performed using the RIGOL L3000 High Performance Liquid Chromatography (HPLC), equipped with a RIGOL L 3500 UV–V is detector and a Hewlett Packard 1046 fluorescence detector. PAHs concentrations in sediment samples are presented as µg/kg dw (dry-weight) and as ng/L in water samples. The list of PAHs and their abbreviations are presented in Table S3 (Supplementary Information).

2.4 Quality control and Quality assurance

In order to reduce any contamination, all glassware was heated to 200°C before being thoroughly cleaned by acetone, methanol and dichloromethane before their use. The analytical method validation was performed by blank samples, sample duplicates, reference materials (IAEA-417 and IAEA-406), sample spiked with surrogate standards (Pyr-D10, lot:10510 semi volatile internal standards). Pyr-D10 was used as internal standard for the calibration of all of PAHs. Limit of detection (LOD) of PAHs were determined with a signal/noise ratio (S/N) of three. N-hexane and Chr were used as solvent blank with three replicates. None of the 16 targeted PAHs were found in the blank samples. The recovery percentages for the PAHs in water samples and sediment samples ranged between 94–98% and 88–97%, respectively, which are within the acceptable ranges. The PAHs LOD for sediment and water varied between 0.05-0.70 µg/kg and 0.50-1.20 ng/L, respectively.

2.5 Statistical analyses and Models

The data analysis was carried out using IBM SPSS Statistics 26.0. The normality of all PAHs was assessed using Shapiro-Wilk test: the data were not normally distributed and hence were analyzed using nonparametric statistical analysis. The spatial distribution of PAHs was discerned using ArcMap 10.5 (ESRI, USA). PMF (Positive Matrix Factorization) receptor model (released via USEPA, version 5.0) and SOM (self-organizing map), k-Means and Davies-Bouldin index were employed (using MATLAB R2022a) to recognize the origins of PAHs and estimate the contributions of different origins via their fingerprints (Li et al., 2018).

2.5.1 PMF (Positive Matrix Factorization) Method

The PMF method executed non-negative constraints as a superior receptor model to identify the different sources of PAHs and quantify the contributions based on their chemical and distributional fingerprints. The advantages of the PMF model for source apportionment in comparison with other models are the usage of nonnegativity constraints and better efficiency in contributions and solution the factor profiles with user provided uncertainties via weighing each single value (Yang et al., 2018; Li et al., 2022).

EPA PMF 5.0 User Guide and Fundamentals, describes the PMF Model (USEPA, 2014). Briefly, the purpose of multivariate model is to resolve the chemical mass balance by decomposing a matrix of input data into factor profiles (f = p × n) and origins contributions
(g = m × p). The model controls factor profiles and origins contributions to get the most appropriate solution via minimizing the objective function (Q) presented in Eq. 1.

$$Q = \sum_{i=1}^{m} \sum_{j=1}^{n} \left[\frac{xji - \sum_{k=1}^{p} g_{ik} f_{kj}}{U_{ij}}\right]^2 \qquad (1)$$

where, Q is the weighted sum of squares of residuals; m and n are the number of samples and number of species, respectively; xij is the concentration of species j detected in sample i; p is the factors number defined by users; g_{ik} is the contribution of k^{th} source in sample i; f_{kj} is the concentration of species j in the k^{th} origin; U_{ij} is the species j uncertainty for i^{th} sample (Wang et al., 2016; Cao et al., 2020). PAHs concentrations in samples less than the limit of detection (LOD) were substituted as the half of LOD and the uncertainty value (U) was computed using 5/6 of LOD. For the PAH concentrations greater than LOD, the U value was computed as outlined in (Eq. 2) in Zhang et al (2021):

$$\text{U value} = \sqrt{(\text{Error Fraction} \times \text{concentration})^2 + (0.5\times \text{LOD})^2} \qquad (2)$$

Where error fraction is the evaluation uncertainty (10%) obtained by analyzing standard and duplicate samples. (USEPA, 2014; Bi et al., 2018).

2.5.2 SOM (Self-Organizing Map) Method

Kohonen's self-organizing map (SOM) has been widely used for feature detection, dimension reduction, clustering and environmental classification (Gu et al., 2019; Bhuiyan et al., 2021). This statistical tool is an artificial neural network that uses an unsupervised competitive learning method and visualizes a two-dimensional space of high-dimensional dataset that consists of units (neurons) and the topological relationship between input data dependably converted to a geometric relationship (Kohonen, 1990; Yang et al., 2021). In this work, SOM was employed for identification of patterns in the distribution of PAHs in Miankaleh sediment samples. The component planes show the graphical examination of relations between variables. Sampling site clustering could be used to find out local sediment state characteristics and simplify sediment sources management via adopting strategies based on similarities of sediment quality (Gu et al., 2019).

SOM could be applied only for the imaging goal whenever ignoring its clustering capability. Although usually, it performs the clustering and visualization concurrently, the similar to the mixture of Q-mode and R-mode cluster analysis methods (Bhuiyan et al., 202; Li et al., 2018). The Kohonen training algorithm makes a result of arranged neurons on a topological map connected through a neighborhood relation (Dai et al., 2018; Guo et al., 2020). Unlike PCA, SOM is capable of handling complex and nonlinear problems. It can manage outliers and missing data and noise have no effect on results because of sampling or measurement errors. Though there are no special method to determine the size of the SOM, it was determined via the following equation (Eq. 3) described by Li et al (2018):

$$m = 5\sqrt{n} \qquad (3)$$

where n is the analyzed number of sample (in this study n=32) and m is close to the neurons number. The optimal size of SOM ≈ 28, assuming this supposition is correct. To better choose the optimal map size, we trained the networks at various sizes (25 to 35) and also, we assessed the quality of the maps using the minimum of the topographical error (TE) and quantization error (QE). For dividing the SOM units into subgroups, we made use of two methods. We determined the subgroup borders between the SOM units via the united distance matrix algorithm (U matrix). k-means clustering was used to the SOM output nodes to affirm the sub-groups separated via the U matrix. This manner is efficient for SOM clustering. The Davies-Bouldin index was used to assess the efficiency of the classification, with the lowest value (Li et al., 2018; Gu et al., 2019).

Table. 2. PAHs concentration in the sediments of Miankaleh Wetland

unit: μg/kg dry weight	P [a]	LOD	Min.	Max.	Mean	Med.	S.D.	C.V.
Nap	0.01	0.70	1.72	68.93	24.17	17.36	18.92	0.78
Flu	0.05	0.10	0.08	7.17	2.31	2.44	1.70	0.74
Phe	0.00	0.20	0.15	54.97	9.79	5.50	11.94	1.22
Ant	0.00	0.10	0.08	7.37	1.75	1.37	1.71	0.97
Fl	0.00	0.10	0.08	10.01	2.38	1.83	2.14	0.90
Pyr	0.00	0.10	0.25	25.65	3.61	1.75	4.79	1.33
BaA	0.00	0.05	0.04	26.37	3.44	2.12	4.64	1.35
Chr	0.00	0.10	0.08	9.46	2.55	1.78	2.20	0.86
BbF	0.00	0.20	0.15	21.07	2.09	0.56	3.75	1.80
BkF	0.00	0.20	0.20	11.46	1.78	1.36	1.97	1.11
BaP	0.00	0.20	0.15	10.92	1.55	1.23	1.87	1.21
InP	0.00	0.30	0.23	12.05	1.71	1.41	2.20	1.29
BghiP	0.00	0.23	0.23	7.84	2.04	1.61	1.99	0.97
∑PAHs			4.54	196.90	59.18	45.06	46.39	0.78
∑ 2-3 rings			2.64	120.77	38.03	29.17	30.79	0.81
∑ 4-6 rings			1.90	105.38	21.15	14.41	20.25	0.96
LMW/HMW			0.44	6.54	2.29	2.02	1.63	0.71

[a] P value calculated by Shapiro-Wilk test

3. Results and Discussion

3.1. PAH in water samples

PAHs concentration in water samples (Fig. 2) changed from 10.61 to 564.28 ng/L with a mean 127.87 ± 148.23 ng/L, with a large difference across the sampling sites (Table 1).

In this study, the concentrations of BkF, Acy, BaA, Ace, BbF, BaP, InP, DahA and BghiP for all water samples were lower than their LOD. Pyr, Chr and Fl composition were identified in most of the water samples in relation to HMW-PAH. A predominant presence of the LMW-PAHs was observed in the water samples because HMW-PAHs are mainly eliminated by sedimentation while LMW-PAHs are often eliminated by dissolution and dilution (Niu et al., 2021). Nap had higher concentrations (Table 1) than other congeners, changing from 1.75 to 512.00 ng/L, with a mean value of 99.52 ng/L followed by Phe (8.81 ng/L) > Pyr (6.09 ng/L) > Flu (4.57 ng/L) > Ant (4.42 ng/L) > Fl (3.24 ng/L) > Chr (1.23 ng/L). The median concentration of individual PAHs is partly similar to the corresponding average concentration (except Nap), indicating that most of the sampling sites have low concentrations of PAHs (Table 1). Coefficients of variation (CV) of ∑PAHs were > 50%, and Nap exceeded 100%, suggesting variation in the PAHs concentrations in the wetland water samples. Based on PAH classification in water described by Li et al (2015) and Ashayeri et al (2018), ∑PAHs determined in Miankaleh Wetland water samples shows low to slight pollution, except for one sampling site that shows moderate pollution (564.28 ng/L) perhaps due to the existence of a large fishing company located close to this site.

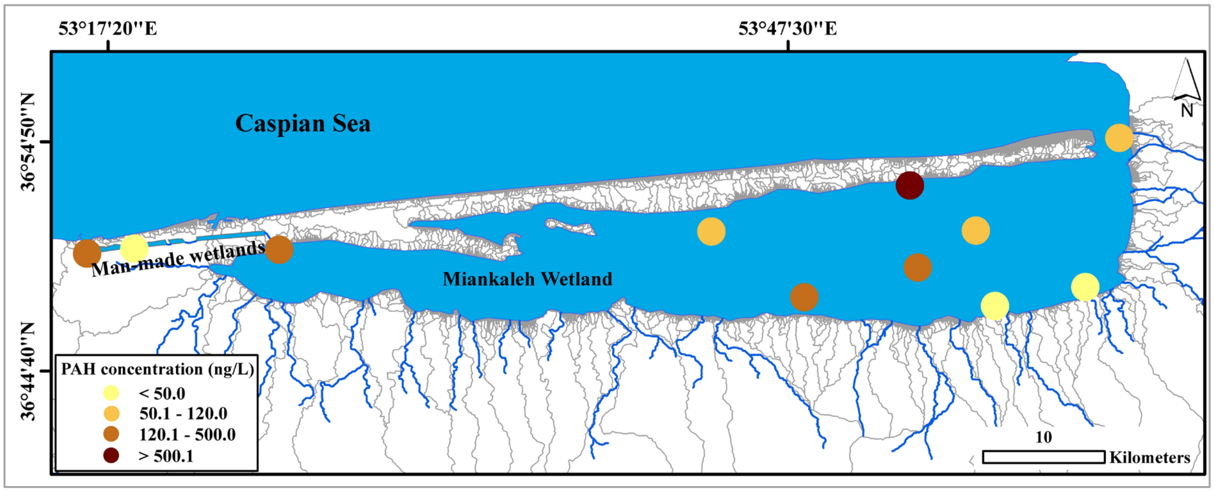

Fig. 2. PAHs concentration in Miankaleh Wetland water.

According to the concentration thresholds specified by the United States Environmental Protection Agency (USEPA, 2015), the Canadian Environmental Quality guidelines (CEQGs, 2015), and EU Marine Strategy Framework Directive (2016), the maximum concentrations of all compounds measured (Flu, Nap, Ant, Fl, Phe, Pyr and Chr) in the wetland water samples did not exceed the corresponding safety thresholds (Table 1).

In comparison to other wetlands in Iran, the PAHs concentration observed in this work are higher than those reported for Alagol, Almago and Agigol wetlands (19 to 112 ng/L., Taheri Azad et al., 2009), Hoor Al-Azim wetland (15.30 to 160.15 ng/L., Sheikh Fakhradini et al., 2019) and Shadegan wetland (42 ± 2.30 to 136 ± 7.50 ng/L., Ashayeri et al., 2018). When compared to other polluted wetlands, PAHs in dissolved phase from Miankaleh Wetland are considerably lower than those found in coastal wetlands (Yellow River-Delta) (295 to 1452 ng/L., Zhang et al., 2015), and Beidagang Wetland in Tianjin, China (73500 to 164000 ng/L., Wang et al., 2020). The PAH levels found in present work are close to those of the unpolluted constructed wetland Tianjin, China (114 to 443 ng/L., Chen et al., 2021). The PAHs concentration in water of Miankaleh Wetland displayed no correlation with DO, EC, Eh and temperature (Table S4, Supplementary Information). Partitioning of PAHs between water and particulate matter (sediments and suspended material) could be influenced by pH (Bi et al., 2018), but the negative correlation between concentration of PAHs and pH here is more associated with the pH of surface runoff input. Large amounts of surface runoff input (with low pH) would cause high level of PAHs in Miankaleh Wetland water.

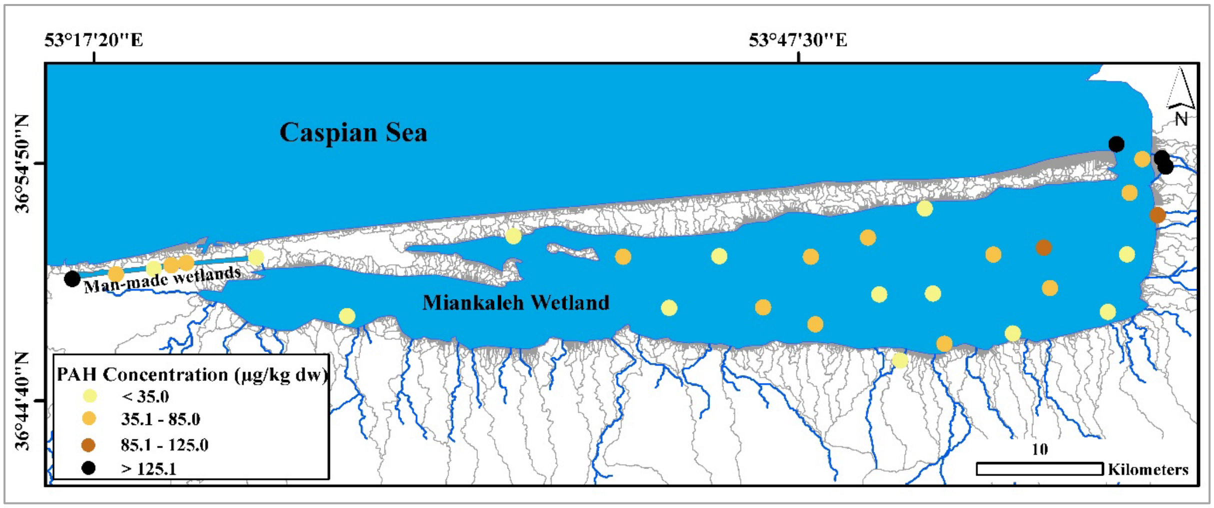

Fig.3. PAHs concentration in Miankaleh Wetland sediments.

3.2. PAHs in sediment samples

The concentrations of ∑PAHs detected in the Miankaleh Wetland sediments are illustrated in Fig. 3. The highest concentrations were close to Chopoghli channel (affected by municipal and industrial sewage discharges, port activities and transport emissions) and Zaghmarz Lapoo (affected by Neka port and powerplant) (Fig. 1). PAHs concentrations in the Miankaleh Wetland sediments changed from 4.54 to 196.90 µg/kg dw with a mean of 59.18 ± 46.39 µg/kg dw (Table 2). Concentrations of PAHs (except Ace, Acy and DahA) for all sediment samples were more than their respective LOD. The median of individual PAHs is lower than the respective average concentration, indicating most sites contain relatively low PAH concentrations, similar to the water samples. The highest concentration recorded was for Nap (1.72–68.93 µg/kg dw, with mean concentration of 24.17 µg/kg dw), followed by the mean concentrations of other compounds (Pyr, BaA, Chr, Fl, Flu, Phe, BbF, BghiP, BkF, InP, Ant and BaP) changing from 1.55 to 9.79 µg/kg dw. In this study, LMW-PAHs dominate at most sites. Pyrogenic sources are often responsible for HMW-PAHs by combustion processes. Petrogenic origins often increase LMW-PAHs via releasing fuel oil or light refined petroleum products. Therefore, the HMW/LMW ratio could be used to specify the sources of PAHs (Chen et al., 2020a). The dominance of LMW-PAHs also affirms a recently generated or local sources of PAHs (oil leaks and fuel from boat engines and sewage discharge), since LMW-PAHs are more unstable, degrade and evaporate more quickly than HMW-PAHs (Wang et al., 2019; Jahromi et al., 2020).

The PAHs concentrations in the Miankaleh Wetland sediment samples are lower than those in Shadegan wetland (0 ± 0.50 to 317 ± 14.30 µg/kg dw., Ashayeri et al., 2018), Anzali wetland (212 to 9009 µg/kg dw., Yancheshmeh et al., 2014), Hoor Al-Azim wetland (15.78 to 410.20 µg/kg dw., Sheikh Fakhradini et al., 2019) and Al-Hawizah wetland (1071 to 15540 µg/kg dw., Janadeleh et al., 2018). The PAH residual concentrations are higher than those in previous work in this region (Gorgan Bay), aquatic ecosystem of Miankaleh Wetland (13.70 to 23.68 µg/kg dw., Zafarani et al., 2022). Future industrial activities in this region have the potential to increase the level of PAHs. Also, as Miankaleh Wetland is linked to the Caspian Sea, the PAHs level in this wetland is compared with those reported in the southern sediment samples of the Caspian Sea. The results indicate that PAH residual levels in the sediment samples of

Miankaleh Wetland are lower than those in Caspian Sea offered by Baniemam et al. (2017) in fall season (17.30 to 926.70 μg/kg dw) and similar to those in Caspian Sea in winter season (14.30 to 85.80 μg/kg dw). All PAHs concentrations in Caspian Sea in the winter were lower than sediment quality guidelines/thresholds. Hence, there is no threat to aquatic organisms (Baniemam et al., 2017). A comparison of PAHs concentration in the sediment samples of this study with those reported from other wetlands worldwide reveals that PAH levels in the sediments of Miankaleh Wetland are less than the PAH levels in sediments of estuarine wetland and tidal flat wetlands of the Bohai coast region (ranging from 51.10 to 2332.80 μg/kg dw and 40.40 to 688.50 μg/kg dw., Xu et al., 2019), Qinhuangdao coastal wetland (341.61 to 4703.80 μg/kg dw., Lin et al., 2018), Liaohe River Delta wetland, Northeast China (46 to 1167 μg/kg dw., Ma et al., 2017), coastal wetlands of the Yellow River Delta, China (1013 to 2011 μg/kg dw., Zhang et al., 2015), Sundarban mangrove wetland of India and Bangladesh (208.30 to 12993.10 μg/kg dw., Zuloaga et al., 2013). The PAHs concentrations in the sediments of this study are similar to mangrove wetlands (coastal wetlands) in South Atlantic subtropical (<LOD – 234.30 μg/kg dw., Garcia and Martins, 2021) and estuarine and coast of CanGio wetland, Vietnam (31-112 μg/kg dw., Thuy et al., 2021). Miankaleh Wetland Sediments are classified as having low to moderate levels of pollution (at 0-100 and 100–1000 μg/kg dw; He et al., 2016, Niu et al., 2021).

The sediment composition especially organic matter is known to be an important factor for PAHs retention in sediments (Hadibarata et al., 2019). Table S5 (Supplementary Information) shows the correlation coefficients between the concentration of PAHs and sediment parameters. There was no significant correlation between the concentration of PAHs and sediment parameters. These results are similar to those offered in previous studies indicating poor correlation between the PAHs concentrations and sediment parameters (Hadibarata et al., 2019). Furthermore, source of PAHs could describe the distribution and concentration of PAHs and both PAHs distribution and concentration are often controlled by direct inputs (Sheikh Fakhradini et al., 2019).

3.3 Water-Sediment partitioning of PAHs

Water-Sediment partitioning affects aquatic environment quality specially when understanding the fate and transport of PAHs composition in an aquatic ecosystem is concerned. The fugacity fraction (ff) approach was applied in Miankaleh Wetland to evaluate and assess the separation of PAHs composition among water and sediments. The fugacity fraction was computed to assess the exchange behavior and balanced status of PAHs between water and sediment through the Eq. 4, 5 and 6, described by Zhao et al (2021a):

$$\mathrm{ff} = \mathrm{K'_{OC}} / (\mathrm{K'_{OC}} + \mathrm{K_{OC}}) \qquad (4)$$

$$\mathrm{K'_{OC}} = \mathrm{C_S} / (\mathrm{C_W} \times \mathrm{f_{OC}}) \qquad (5)$$

$$\mathrm{f_{OC}} = \mathrm{f_{OM}} / 1.8 \qquad (6)$$

where K'_{OC} (mL/g) is the in-place water-sediment partitioning coefficient., K_{OC} (mL/g) is the partitioning coefficient of organic carbon normalized; C_s (ng/g dw) is the PAHs concentration in solid phase; C_W (ng/L) is the PAHs concentration in aqueous phase; f_{OC} (no unit) is the organic carbon fraction in solid and f_{OM} (%) is the organic material fraction in solid (Zhao et al 2021a). A value of ff < 0.30 indicates that the sediment acts as a sink for PAHs, PAHs are in water and sediment equilibrium when ff 0.30 < ff < 0.70, whereas ff > 0.70 indicates the sediment acts as a secondary source for PAHs (Chen et al., 2020b, Jia et al., 2021). In this work, the ff values for PAHs (except Chr) were lower than 0.30, displaying a flux from water to sediment (Table 3). Although, the ff values of Chr are in the range of 0.08-0.76, suggesting a balanced status between water and sediment. It is necessary to consider the fact that sampling was done in a dry season. Thus, the results are reflective of the dry season.

Table 3. The partitioning coefficient of organic carbon normalized (Log K_{OC}), Fugacity fraction (ff) and the potential of water-sediment partition of PAHs in Miankaleh Wetland

Compounds	Log K_{OC} (ml/g) [a]	Fugacity fraction (ff)				Water-sediment partition potential (%) [b]		
		Min.	Max.	Mean	S.D.	Sink	Balance	Source
Nap	3.11	0.01	0.33	0.13	0.11	72.73	27.27	0.00
Flu	5.22	0.01	0.26	0.13	0.09	63.64	36.36	0.00
Phe	4.42	0.01	0.46	0.22	0.15	54.55	45.45	0.00
Ant	4.41	0.01	0.31	0.12	0.11	72.73	27.27	0.00
Fl	4.15	0.01	0.47	0.16	0.14	72.73	27.27	0.00
Pyr	4.64	0.02	0.39	0.16	0.11	90.91	9.09	0.00
Chr	5.45	0.08	0.76	0.47	0.22	27.27	63.64	9.09

[a] log K_{OC}: the partitioning coefficient of organic carbon normalized of PAHs ml/g (Zhao et al., 2021a).
[b] Water-sediment partition potential (%): the percent of samples with ff < 0.30, ff 0.30 to 0.70 and ff > 0.70.

3.4 Source apportionment of PAHs

3.4.1 PMF Method

Sediments are a useful and long-term archive of PAHs contamination (Zhang et al., 2022). The results of sediment samples were applied to identify the possible sources of PAHs in the Miankaleh Wetland. The concentrations of 13 PAHs from 32 stations were used for the PMF method as input data. Two to five factors were examined in random seed mode with 100 base runs to assure that the minimum of Q is found and to decide the optimal number of factors. Finally, three factors were specified according to the guidelines outlined in Kamiya et al. (2016) and Leong et al. (2017), where Q (true) ≈ Q (robust) and strong correlation between observation and prediction, with most standardized residuals between -3 and +3. In the model, all of PAHs had strong correlations (r^2>0.85), excepted Phe and Flu due to their weak correlation with the predicted value (r^2=0.55 and 0.43 respectively). The mean ratio of Q (robust) / Q (true) was 0.95 and the results of error assessment by employing the displacement (DISP), the bootstrap (BS) (with the boot factor values over 96%) and the bootstrap-displacement (BS-DISP) methods offered no factor swaps present for dQmax=3, indicating the factor profiles were permanent after application of the constraints, so the number of factors is appropriate in this study. The PMF 5, offers the rotational freedom parameter (F-peak) function that controls whether more extreme values are supposed for factor loadings (F-peak>0) or factor scores (F-peak<0). Here, modifying the F-peak value did not result in significantly better source profiles, and so base run results (F-peak=0) are reported.

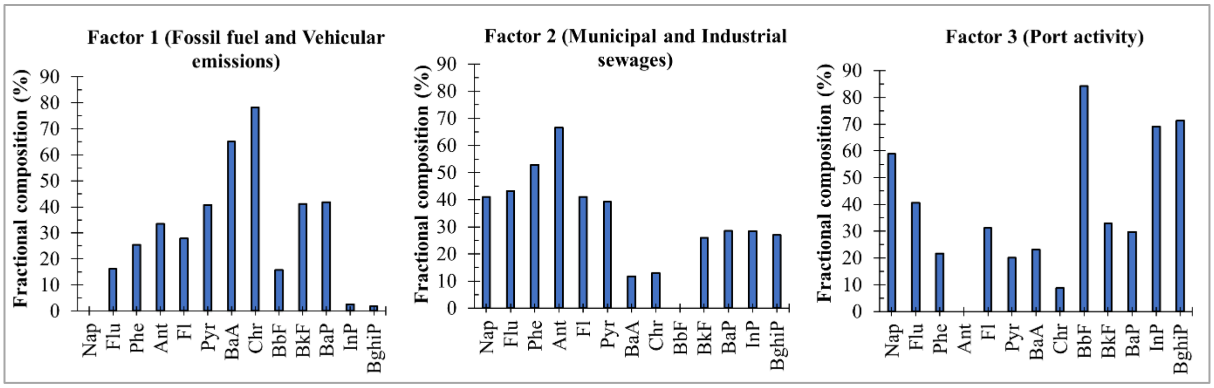

Fig.4. Factor composition of PAHs in the Miankaleh Wetland sediments via the PMF method.

The PAHs in the sediments of Miankaleh Wetland are classified into three categories (Fig. 4). The first category is highly loaded by high-molecular weight (4 or 5-rings) PAHs like combustion PAHs (BaA, BkF, Pyr and BaP), which are typical markers for fossil fuel and vehicular emissions (boat traffic), including gasoline and diesel engine emissions (Davis et al., 2019) and Chr acts as marker for coal combustion, industrial boiler and residential heating (similar with BkF) (Yang et al., 2018; Cao et al., 2020). As a consequence, Factor 1 (with 30% of the total factor contribution) was selected to represent the fossil fuel and vehicular emissions. The second category is dominated by LMW-PAHs (2 or 3-rings) like Nap, Ant, Flu, Phe and Fl (4-ring). As LMW-PAHs are important indicator of petrogenic source that originate from the volatilization of related products to petroleum (Yang et al., 2018), so we concluded that the input of petrogenic PAHs to Miankaleh Wetland (Factor 2) could be associated with municipal and industrial wastewater which enters by runoff or direct discharges into the wetland. Factor 2 computed for 32.2% of the total factor contribution. The final pattern grouped high-molecular weight BbF, BghiP, InP (5 and 6-rings) PAHs that are combustion PAHs (Davis et al., 2019), and Nap (2-ring PAH) that mainly come from leakage and volatilization due to oil production activities (Liu et al., 2021). Also, the results of PAHs in sediment of South of Caspian Sea by Baniemam et al. (2017) indicated that PAHs in sediment samples mostly come from petroleum and petroleum combustion. Therefore, Factor 3 (accounting for 37.8% of the total factor contribution) is considered with prevalence of petrogenic influence and petroleum-related activities consistent with port activity near Miankaleh Wetland.

Overall, the PMF method analysis indicated that fossil fuel and vehicular emissions (Factor 1), municipal and industrial sewages (Factor 2) and port activity (Factor 3) contribute for 30, 32.2 and 37.8 % of the ΣPAHs, respectively (Fig. 4).

The TE and QE were estimated at various map sizes (Table S6, Supplementary Information). According to the minimum of TE and QE and attempting to keep away from a large number of blank output neurons that were not ever chosen as a winner (Li et al., 2018), we found that 34 (17 × 2) units is the most appropriate map size. The Davies-Bouldin index reached its minimum value for three clusters (Fig. 5a), and the k-means algorithm separated the output neurons into three clusters (I–III). On the two-dimensional map by appointing the sample number to its nearest output neuron (i.e., BMU) each sample was partitioned to the same cluster in the original data as its BMU. Of all 32 sites, 6 sites were located in cluster I, 17 sites were located in cluster II and 9 sites were grouped in cluster III (Fig. 5b). Alternatively, the U matrix was applied to cluster the trained SOM units. We identified three clusters on the map. The U matrix and relative component plane of the ΣPAHs in the Miankaleh Wetland obtained by the SOM analysis are illustrated in Fig. 6. SOM planes show the importance of delivered variables for each SOM unit in color ranks where a similar color specified a positive correlation between variables, whereas different colors displayed negative correlations (Bhuiyan et al., 2021). Nap was highly concentrated at the right, which is quite similar to Phe, Flu, Ant and Fl in the component plane. Pyr, BaA, Chr, BkF and BaP showed a similar pattern of concentration. Moreover, in terms of higher concentrations, significant relations were observed among BbF, InP and BghiP indicating a common association among the variables.

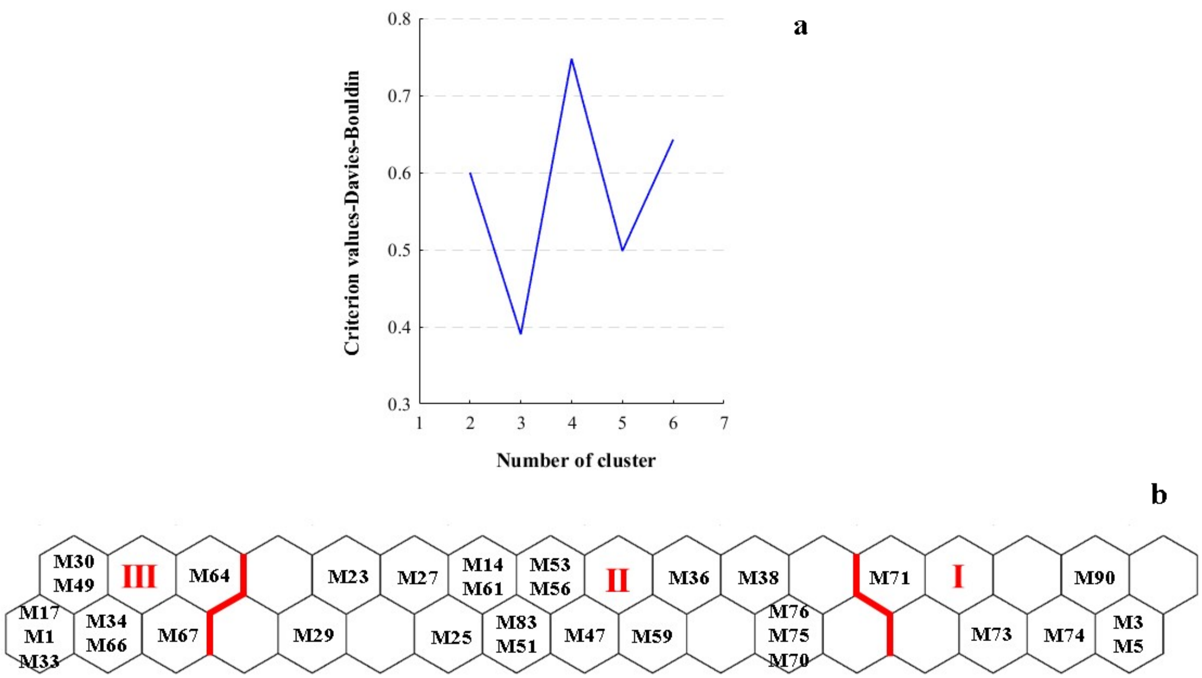

Fig.5. Evaluation of optimal number of clusters by plot of Davies-Bouldin index (a) and patterns of sampling site clustering in sediments (b).

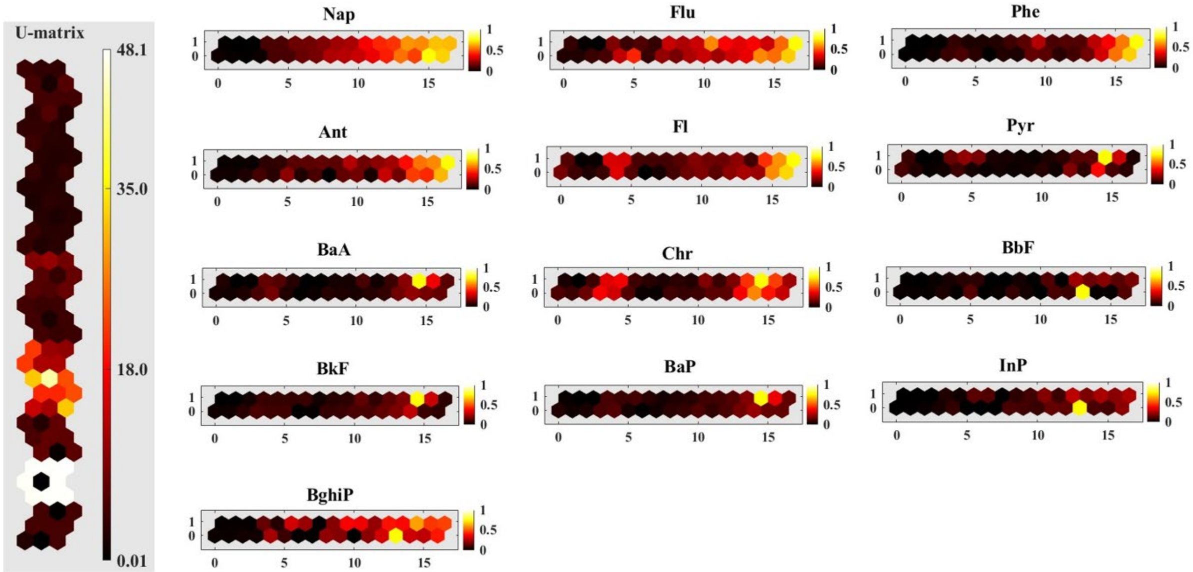

Fig.6. U-matrix and SOM map of concentration of PAHs in sediment.

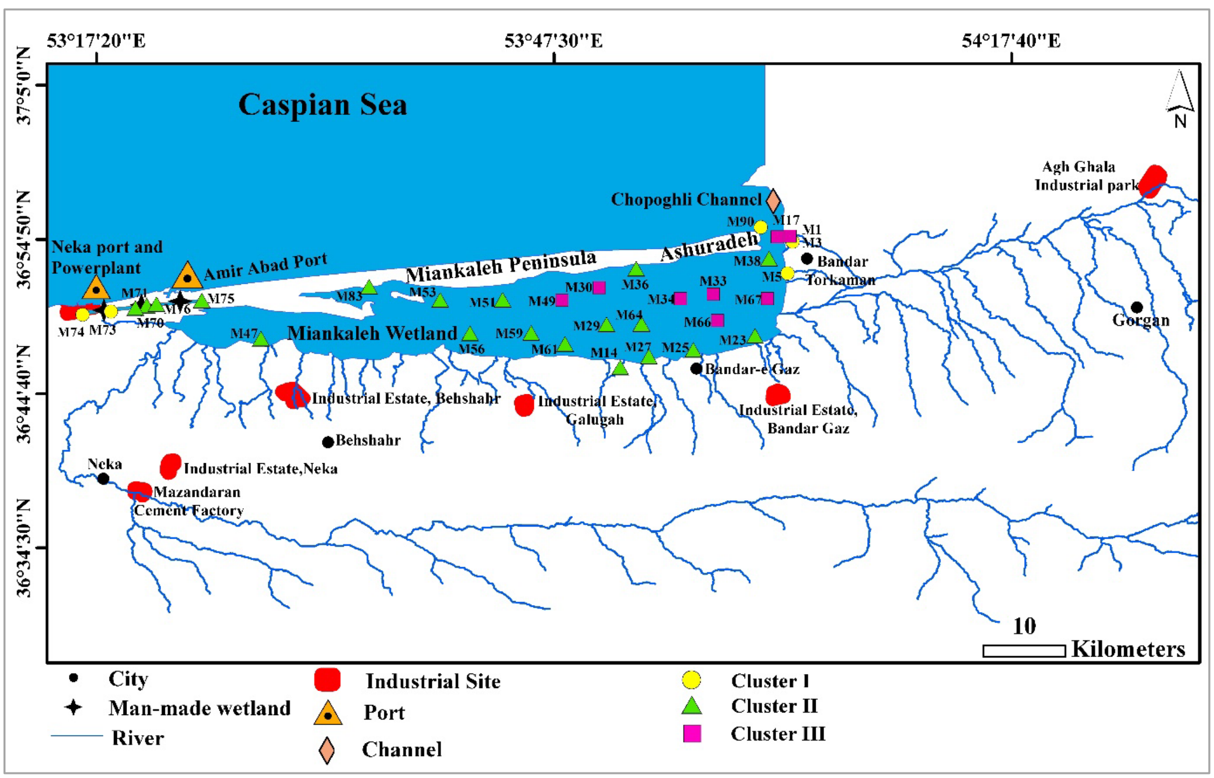

Fig.7. Spatial distributions of the sampling site clustering by SOM.

Also, the SOM algorithm was applied to clustering the sampling sites. Cluster I and III were distributed in a geographically limited region. Fig. 7 illustrates the spatial distribution of the three clusters in the study region. As predicted, sites that had similar PAH components and were geographically close to some sources, occur in the same cluster. For example, Cluster III is located around the Chopoghli channel (see

Fig. 1) and samples in this cluster have high concentration of combustion PAHs (BbF, BghiP, InP (5 and 6-ring) and Nap (2-ring PAH) and can be related to oil and by product spills from human activities (de Almeida et al., 2018; Liu et al., 2021). Cluster II is located in a wider geographical area compared with other two clusters, mainly affected by petrogenic source (2-or 3-ring PAHs) commonly considered as important indicator of volatilization of petroleum products (Yang et al., 2018). Cluster 1 includes combustion PAHs like Pyr, Chr, BaA, BkF and BaP which are mainly known to be markers of combustion of fossil fuels and vehicular sources (Yang et al., 2018; Azimi-Yancheshmeh et al., 2021). These results are similar to the results obtained via the PMF model.

4. Conclusion

The government of Iran's strategic mission regarding the Miankaleh International Wetland includes environmental protection and economic development, and therefore a comprehension of the pollution status is especially essential to identify major environmental problems resulting from human activities. According to the fact that lack of management and control of the conditions of this sensitive ecosystem, will lead to repeated bird losses in the coming years and also based on importance of this wetland in terms of fishing and Caviar, it is important to investigate and monitor the extent, degree and source of every kind of pollutants in this wetland. This study investigated the concentrations of 16 priority PAH and their pollution level, fugacity fraction (ff) and PAHs source apportionment in Miankaleh Wetland, southeast of the Caspian Sea. The major findings in this study include (i) most water and all sediment samples show low to slight pollution and low to moderate pollution, respectively. The determined concentrations of Acy, Ace, BbF, BaP, InP, BkF, BaA, BghiP and DahA in all water samples and Acy, Ace and DahA in all sediment samples were lower than their LODs. However, when higher concentrations of PAHs observed in this study are compared with previous results in the aquatic ecosystem of Miankaleh Wetland it becomes clear that PAHs pollution input is still occurring and shows an increasing trend; (ii) based on the estimated fugacity fraction (ff), sediments were found to act as a sink for most PAHs and they do not act as a secondary source yet; (iii) PAH contamination does not seem to be a likely contributor to the deaths of the migratory birds. To deal with this threat to the avifauna, attention may then be focused on factors such as nature and rate of sediment; (iv) fossil fuel and vehicular emissions, municipal and industrial sewages and port activity are the three main contributors of PAH in Miankaleh Wetland. From the point of view of human activity, controlling vehicular and power plant emissions and treating sewage can assist source-oriented PAH mitigation.

Acknowledgement

The authors thank the Research Committee and Medical Geology Center of Shiraz University for logistical assistance. Thanks also to the Research Center for Environmental and Sustainable Development (RCESD) of Iranian Department of Environment for making this research feasible.

Author Contributions Statement

All authors contributed to the study conception and design. Mahsa Rokhbar: Investigation, Writing – original draft, Conceptualization, Formal analysis. Behnam Keshavarzi: Supervision, Conceptualization, Project administration, Resources, Reviewing and Editing. Farid Moore: Supervision, Project administration, Resources, Reviewing and Editing. Mehdi Zarei: Investigation, Project administration. Peter S. Hooda: Reviewing and Editing. Michael J. Risk: Reviewing and Editing.

References

Abbasi, S., Keshavarzi, B., Moore, F., Shojaei, N., Sorooshian, A., Soltani, N., Delshab, H. (2019). Geochemistry and environmental effects of potentially toxic elements, polycyclic aromatic hydrocarbons and microplastics in coastal sediments of the Persian Gulf. Environmental Earth Sciences, 78(15), pp.1-15. https://doi.org/10.1007/s12665-019-8420z.

Ashayeri, N. Y., Keshavarzi, B., Moore, F., Kersten, M., Yazdi, M., Lahijanzadeh, A. R. (2018). Presence of polycyclic aromatic hydrocarbons in sediments and surface water from Shadegan wetland–Iran: a focus on source apportionment, human and ecological risk assessment and sediment-water exchange. Ecotoxicology and Environmental Safety, 148, pp.1054-1066. https://doi.org/10.1016/j.ecoenv.2017.11.055.

Alipour, H., Pourkhabbaz, A., Hassanpour, M. (2015). Estimation of potential health risks for some metallic elements by consumption of fish. Water Quality, Exposure and Health, 7(2), pp.179-185. https://doi.org/10.1007/s12403-014-0137-3.

Ambade, B., Sankar, T. K., Kumar, A., Gautam, A. S., Gautam, S. (2021 a). COVID-19 lockdowns reduce the Black carbon and polycyclic aromatic hydrocarbons of the Asian atmosphere: source apportionment and health hazard evaluation. Environment, Development and Sustainability, 23(8), pp.12252-12271. https://doi.org/10.1007/s10668-020-01167-1.

Ambade, B., Sethi, S. S., Kumar, A., Sankar, T. K., Kurwadkar, S. (2021 b). Health risk assessment, composition, and distribution of polycyclic aromatic hydrocarbons (PAHs) in drinking water of Southern Jharkhand, East India. Archives of environmental contamination and toxicology, 80(1), pp.120-133. https://doi.org/10.1007/s00244-020-00779-y.

Ambade, B., Sethi, S. S., Kurwadkar, S., Kumar, A., Sankar, T. K. (2021 c). Toxicity and health risk assessment of polycyclic aromatic hydrocarbons in surface water, sediments and groundwater vulnerability in Damodar River Basin. Groundwater for Sustainable Development, 13, p.100553. https://doi.org/10.1016/j.gsd.2021.100553.

Ambade, B., Kurwadkar, S., Sankar, T. K., Kumar, A. (2021 d). Emission reduction of black carbon and polycyclic aromatic hydrocarbons during COVID-19 pandemic lockdown. Air Quality, Atmosphere & Health, 14(7), pp.1081-1095. https://doi.org/10.1007/s11869-021-01004-y.

Azimi-Yancheshmeh, R., Moeinaddini, M., Feiznia, S., Riyahi-Bakhtiari, A., Savabieasfahani, M., van Hullebusch, E. D., Lajayer, B. A. (2021). Seasonal and spatial variations in atmospheric PM2. 5-bound PAHs in Karaj city, Iran: Sources, distributions, and health risks. Sustainable Cities and Society, 72, pp.1-13. https://doi.org/10.1016/j.scs.2021.103020.

Bagheri, T., Gholizadeh, M., Abarghouei, S., Zakeri, M., Hedayati, A., Rabaniha, M., Aghaeimoghadam, A. Hafezieh, M. (2020). Microplastics distribution, abundance and composition in sediment, fishes and benthic organisms of the Gorgan Bay, Caspian Sea. Chemosphere, 257, p.127201. https://doi.org/10.1016/j.chemosphere.2020.127201.

Baniemam, M., Moradi, A. M., Bakhtiari, A. R., Fatemi, M. R., Khanghah, K. E. (2017). Seasonal variation of polycyclic aromatic hydrocarbons in the surface sediments of the southern Caspian Sea. Marine pollution bulletin, 117(1-2), pp.478-485. https://doi.org/10.1016/j.marpolbul.2017.01.027.

Bhuiyan, M. A. H., Karmaker, S. C., Bodrud-Doza, M., Rakib, M. A., Saha, B. B. (2021). Enrichment, sources and ecological risk mapping of heavy metals in agricultural soils of dhaka district employing SOM, PMF and GIS methods. Chemosphere, 263, p.128339. https://doi.org/10.1016/j.chemosphere.2020.128339.

Bi, C., Wang, X., Jia, J., Chen, Z. (2018). Spatial variation and sources of polycyclic aromatic hydrocarbons influenced by intensive land use in an urbanized river network of East China. Science of the Total Environment, 627, pp.671-680. https://doi.org/10.1016/j.scitotenv.2018.01.272.

Bianco, F., Race, M., Papirio, S., Esposito, G. (2020). Removal of polycyclic aromatic hydrocarbons during anaerobic biostimulation of marine sediments. Science of The Total Environment, 709, p.136141. https://doi.org/10.1016/j.scitotenv.2019.136141.

Cai, Y., Liang, J., Zhang, P., Wang, Q., Wu, Y., Ding, Y., Wang, H., Fu, C. Sun, J. (2021). Review on strategies of close-to-natural wetland restoration and a brief case plan for a typical wetland in northern China. Chemosphere, 285, p.131534. https://doi.org/10.1016/j.chemosphere.2021.131534.

Canadian Council of Ministers of the Environment (CCME), 2015. Canadian environmental quality guidelines. https://www.ccme.ca/en/summary-table.

Cao, Y., Xin, M., Wang, B., Lin, C., Liu, X., He, M., Lei, K., Xu, L., Zhang, X., Lu, S. (2020). Spatiotemporal distribution, source, and ecological risk of polycyclic aromatic hydrocarbons (PAHs) in the urbanized semi-enclosed Jiaozhou Bay, China. Science of The Total Environment, 717, p.137224. https://doi.org/10.1016/j.scitotenv.2020.137224.

Chen, J., Liao, J., Wei, C. (2020 a). Coking wastewater treatment plant as a source of polycyclic aromatic hydrocarbons (PAHs) in sediments and ecological risk assessment. Scientific reports, 10(1), pp.1-8. https://doi.org/10.1038/s41598-020-64835-2.

Chen, C. F., Ju, Y. R., Su, Y. C., Lim, Y. C., Kao, C. M., Chen, C. W., Dong, C. D. (2020 b). Distribution, sources, and behavior of PAHs in estuarine water systems exemplified by Salt River, Taiwan. Marine pollution bulletin, 154, p.111029. https://doi.org/10.1016/j.marpolbul.2020.111029.

Chen, Z., Ren, G., Ma, X., Zhou, B., Yuan, D., Liu, H., Wei, Z. (2021). Presence of polycyclic aromatic hydrocarbons among multi-media in a typical constructed wetland located in the coastal industrial zone, Tianjin, China: Occurrence characteristics, source apportionment and model simulation. Science of The Total Environment, 800, p.149601. https://doi.org/10.1016/j.scitotenv.2021.149601.

Cui, L., Li, G., Ouyang, N., Mu, F., Yan, F., Zhang, Y., Huang, X. (2018). Analyzing coastal wetland degradation and its key restoration technologies in the coastal area of Jiangsu, China. Wetlands, 38(3), pp.525-537. https://doi.org/10.1007/s13157-018-0997-6.

Davis, E., Walker, T. R., Adams, M., Willis, R., Norris, G. A., Henry, R. C. (2019). Source apportionment of polycyclic aromatic hydrocarbons (PAHs) in small craft harbor (SCH) surficial sediments in Nova Scotia, Canada. Science of the Total Environment, 691, pp.528-537. https://doi.org/10.1016/j.scitotenv.2019.07.114.

de Almeida, M., do Nascimento, D. V., de Oliveira Mafalda Jr, P., Patire, V. F., de Albergaria-Barbosa, A. C. R. (2018). Distribution and sources of polycyclic aromatic hydrocarbons (PAHs) in surface sediments of a Tropical Bay influenced by anthropogenic activities (Todos os Santos Bay, BA, Brazil). Marine pollution bulletin, 137, pp.399-407. https://doi.org/10.1016/j.marpolbul.2018.10.040.

Dai, L., Wang, L., Li, L., Liang, T., Zhang, Y., Ma, C., Xing, B. (2018). Multivariate geostatistical analysis and source identification of heavy metals in the sediment of Poyang Lake in China. Science of the total environment, 621, pp.1433-1444. https://doi.org/10.1016/j.scitotenv.2017.10.085.

Du, J., Jing, C. (2018). Anthropogenic PAHs in lake sediments: a literature review (2002–2018). Environmental Science: Processes & Impacts, 20(12), pp.1649-1666. https://doi.org/10.1039/C8EM00195B.

EU Marine Strategy Framework Directive. https://www.gov.uk/government/publications/list-of-chemicals-for-water-framework-directive-assessments.

Frena, M., Santos, A. P. S., Santos, E., Silva, R. P., Souza, M. R., Madureira, L. A., Alexandre, M. R. (2016). Distribution and sources of sterol biomarkers in sediments collected from a tropical estuary in Northeast Brazil. Environmental Science and Pollution Research, 23(22), pp.23291-23299. https://doi.org/10.1007/s11356-016-7744-4.

Garcia, M. R., Martins, C. C. (2021). A systematic evaluation of polycyclic aromatic hydrocarbons in South Atlantic subtropical mangrove wetlands under a coastal zone development scenario. Journal of Environmental Management, 277, p.111421. https://doi.org/10.1016/j.jenvman.2020.111421.

Gao, P., da Silva, E., Hou, L., Denslow, N. D., Xiang, P., Ma, L. Q. (2018). Human exposure to polycyclic aromatic hydrocarbons: Metabolomics perspective. Environment international, 119, pp.466-477. https://doi.org/10.1016/j.envint.2018.07.017.

Gholami, V., Khalili, A., Sahour, H., Khaleghi, M. R., Tehrani, E. N. (2020). Assessment of environmental water requirement for rivers of the Miankaleh wetland drainage basin. Applied Water Science, 10(11), pp.1-14. https://doi.org/10.1007/s13201-020-01319-8.

Gholizadeh, M., Patimar, R. (2018). Ecological risk assessment of heavy metals in surface sediments from the Gorgan Bay, Caspian Sea. Marine pollution bulletin, 137, pp.662-667. https://doi.org/10.1016/j.marpolbul.2018.11.009.

Gu, Q., Hu, H., Ma, L., Sheng, L., Yang, S., Zhang, X., Zhang, M., Zheng, K. Chen, L. (2019). Characterizing the spatial variations of the relationship between land use and surface water quality using self-organizing map approach. Ecological Indicators, 102, pp.633-643. https://doi.org/10.1016/j.ecolind.2019.03.017.

Guo, C., Chen, Y., Xia, W., Qu, X., Yuan, H., Xie, S., Lin, L. S. (2020). Eutrophication and heavy metal pollution patterns in the water suppling lakes of China’s south-to-north water diversion project. Science of The Total Environment, 711, p.134543. https://doi.org/10.1016/j.scitotenv.2019.134543.

Hadibarata, T., Syafiuddin, A., Ghfar, A. A. (2019). Abundance and distribution of polycyclic aromatic hydrocarbons (PAHs) in sediments of the Mahakam River. Marine Pollution Bulletin, 149, p.110650. https://doi.org/10.1016/j.marpolbul.2019.110650.

He, Y., Meng, W., Xu, J., Zhang, Y., Guo, C. (2016). Spatial distribution and potential toxicity of polycyclic aromatic hydrocarbons in sediments from Liaohe River Basin, China. Environmental monitoring and assessment, 188(3), pp.1-10. https://doi.org/10.1007/s10661-016-5201-y.

Isaie Moghaddam, E., Allahdadi, M. N., Ashrafi, A., Chaichitehrani, N. (2021). Coastal system evolution along the southeastern Caspian Sea coast using satellite image analysis: response to the sea level fall during 1994–2015. Arabian Journal of Geosciences, 14(9), pp.1-16. https://doi.org/10.1007/s12517-021-07106-2.

Jahromi, F. A., Moore, F., Keshavarzi, B., Mohebbi-Nozar, S. L., Mohammadi, Z., Sorooshian, A., Abbasi, S. (2020). Bisphenol A (BPA) and polycyclic aromatic hydrocarbons (PAHs) in the surface sediment and bivalves from Hormozgan Province coastline in the Northern Persian Gulf: A focus on source apportionment. Marine Pollution Bulletin, 152, p.110941. https://doi.org/10.1016/j.marpolbul.2020.11094.

Janadeleh, H., Kameli, M. A., Boazar, C. (2018). Seasonal variations of metal pollution and distribution, sources, and ecological risk of polycyclic aromatic hydrocarbons (PAHs) in sediment of the Al Hawizah wetland, Iran. Human and Ecological Risk Assessment: An International Journal, 24(4), pp.886-903. https://doi.org/10.1080/10807039.2016.1277416.

Jia, T., Guo, W., Liu, W., Xing, Y., Lei, R., Wu, X., Sun, S. (2021). Spatial distribution of polycyclic aromatic hydrocarbons in the water–sediment system near chemical industry parks in the Yangtze River Delta, China. Science of The Total Environment, 754, p.142176. https://doi.org/10.1016/j.scitotenv.2020.142176.

Jisha, K. C., Puthur, J. T. (2021). Ecological Importance of Wetland Systems. Wetlands Conservation: Current Challenges and Future Strategies, pp.40-54. https://doi.org/10.1002/9781119692621.ch3.

Kamiya, Y., Iijima, A., Ikemori, F., Okuda, T., Ohura, T. (2016). Source apportionment of chlorinated polycyclic aromatic hydrocarbons associated with ambient particles in a Japanese megacity. Scientific reports, 6(1), pp.1-10. https://doi.org/10.1038/srep38358.

Kheirabadi, H., Noori, R., Samani, J., Adamowski, J. F., Ranjbar, M. H., Zaker, N. H. (2018). A reduced-order model for the regeneration of surface currents in Gorgan Bay, Iran. Journal of Hydroinformatics, 20(6), pp.1419-1435. https://doi.org/10.2166/hydro.2018.149.

Khiari, N., Charef, A., Atoui, A., Azouzi, R., Khalil, N., Khadhar, S. (2021). Southern Mediterranean coast pollution: Long-term assessment and evolution of PAH pollutants in Monastir Bay (Tunisia). Marine Pollution Bulletin, 167, p.112268. https://doi.org/10.1016/j.marpolbul.2021.112268.

Kohonen, T. (1990). The self-organizing map. Proceedings of the IEEE, 78(9), 1464-1480.

Kouhanestani, Z. M., Roelke, D. L., Ghorbani, R., Fujiwara, M. (2019). Assessment of spatiotemporal phytoplankton composition in relation to environmental conditions of Gorgan Bay, Iran. Estuaries and Coasts, 42(1), pp.173-189. https://doi.org/10.1007/s12237-018-0451-2.

Kousali, M., Salarijazi, M., Ghorbani, K. (2022). Estimation of Non-Stationary Behavior in Annual and Seasonal Surface Freshwater Volume Discharged into the Gorgan Bay, Iran. Natural Resources Research, 31(2), pp.835-847. https://doi.org/10.1007/s11053-022-10010-5.

Kumar, S., Islam, A. R. M. T., Hasanuzzaman, M., Salam, R., Khan, R., Islam, M. S. (2021). Preliminary assessment of heavy metals in surface water and sediment in Nakuvadra-Rakiraki River, Fiji using indexical and chemometric approaches. Journal of environmental management, 298, p.113517. https://doi.org/10.1016/j.jenvman.2021.113517.

Lee, C. M., Choi, H., Kim, Y., Kim, M., Kim, H., Hamm, S. Y. (2021). Characterizing land use effect on shallow groundwater contamination by using self-organizing map and buffer zone. Science of the Total Environment, 800, p.149632. https://doi.org/10.1016/j.scitotenv.2021.149632.

Leong, J. Y. C., Chong, M. N., Poh, P. E., Hermawan, A., Talei, A. (2017). Longitudinal assessment of rainwater quality under tropical climatic conditions in enabling effective rainwater harvesting and reuse schemes. Journal of Cleaner Production, 143, pp.64-75. https://doi.org/10.1016/j.jclepro.2016.12.149.

Leroy, S.A.G., Amini, A., Gregg, M.W., Marinova, E., Bendrey, R., Zha, Y., Beni, A.N. Nashli, H.F. (2019). Human responses to environmental change on the southern coastal plain of the Caspian Sea during the Mesolithic and Neolithic periods. Quaternary Science Reviews, 218, pp.343-364. https://doi.org/10.1016/j.quascirev.2019.06.038.

Li, R., Cai, J., Li, J., Wang, Z., Pei, P., Zhang, J., Krebs, P. (2022). Characterizing the long-term occurrence of polycyclic aromatic hydrocarbons and their driving forces in surface waters. Journal of Hazardous Materials, 423, p.127065. https://doi.org/10.1016/j.jhazmat.2021.127065.

Li, P., Cao, J., Diao, X., Wang, B., Zhou, H., Han, Q., Zheng, P. Li, Y. (2015). Spatial distribution, sources and ecological risk assessment of polycyclic aromatic hydrocarbons in surface seawater from Yangpu Bay, China. Marine pollution bulletin, 93(1-2), pp.53-60. https://doi.org/10.1016/j.marpolbul.2015.02.015.

Li, T., Sun, G., Yang, C., Liang, K., Ma, S., Huang, L. (2018). Using self-organizing map for coastal water quality classification: Towards a better understanding of patterns and processes. Science of the Total Environment, 628, pp.1446-1459. https://doi.org/10.1016/j.scitotenv.2018.02.163.

Li, Y., Liu, M., Hou, L., Li, X., Yin, G., Sun, P., Yang, J., Wei, X., He, Y. Zheng, D. (2021). Geographical distribution of polycyclic aromatic hydrocarbons in estuarine sediments over China: Human impacts and source apportionment. Science of The Total Environment, 768, p.145279. https://doi.org/10.1016/j.scitotenv.2021.145279.

Lin, F., Han, B., Ding, Y., Li, Q., Gao, W., Zheng, L. (2018). Distribution characteristics, sources, and ecological risk assessment of polycyclic aromatic hydrocarbons in sediments from the Qinhuangdao coastal wetland, China. Marine Pollution Bulletin, 127, pp.788-793. https://doi.org/10.1016/j.marpolbul.2017.09.054.

Liu, C., Huang, Z., Qadeer, A., Liu, Y., Qiao, X., Zheng, B., Zhao, G. Zhao, X. (2021). The sediment-water diffusion and risk assessment of PAHs in different types of drinking water sources in the Yangtze River Delta, China. Journal of Cleaner Production, 309, p.127456. https://doi.org/10.1016/j.jclepro.2021.127456.

Ma, C., Lin, T., Ye, S., Ding, X., Li, Y., Guo, Z. (2017). Sediment record of polycyclic aromatic hydrocarbons in the Liaohe River Delta wetland, Northeast China: implications for regional population migration and economic development. Environmental Pollution, 222, pp.146-152. https://doi.org/10.1016/j.envpol.2016.12.065.

Maleki, P., Rahman, P., Jafariyan, H., Salmanmahiny, A., Ghorbani, R., Gholizadeh, M., Harsij, M. (2020). The risk assessment of water pollution in the Gorgan Bay catchment using the WRASTIC index. Environmental Nanotechnology, Monitoring & Management, 14, p.100393. https://doi.org/10.1016/j.enmm.2020.100393.

Maken Ali, A. S., Heidarnejad, O., Keshavarz Zamanian, V., Habibi, M., Rabiei, K., Talifar, H., Abdolahi, H. (2020). A Comprehensive Monitoring of The High Mortality Rate of Wild Waterbirds in Miankaleh Wetland in 2020. Veterinary Researches & Biological Products, 33(3), pp.130-139. https://doi.org/10.22092/vj.2020.343532.1736.

Mansoori, J. (2009). The Avian Community of Five Iranian Wetlands, Miankaleh, Fereidoonkenar, Bujagh, Anzali and Lavandevil, in the South Caspian Lowlands. Podoces, 4(1), pp.44 59.

-Mereta, S. T., Lemmens, P., De Meester, L., Goethals, P. L., Boets, P. (2021). The Relative Importance of Human Disturbance, Environmental and Spatial Factors on the Community Composition of Wetland Birds. Water, 13(23), p.3448. https://doi.org/10.3390/w13233448.

Niu, L., Luo, X., Cai, H., Liu, F., Zhang, T., Yang, Q. (2021). Seasonal dynamics of polycyclic aromatic hydrocarbons between water and sediment in a tide-dominated estuary and ecological risks for estuary management. Marine Pollution Bulletin, 162, p.111831. https://doi.org/10.1016/j.marpolbul.2020.111831.

Oja, E. B., Swartz, L. K., Muths, E., Hossack, B. R. (2021). Amphibian population responses to mitigation: Relative importance of wetland age and design. Ecological Indicators, 131, p.108123. https://doi.org/10.1016/j.ecolind.2021.108123.

Parchizadeh, J., Belant, J. L. (2020). Mass mortality of migratory birds in Iran. Science, 367(6483), pp.1203-1204.

Pichler, N., de Souza, F. M., Dos Santos, V. F., Martins, C. C. (2021). Polycyclic aromatic hydrocarbons (PAHs) in sediments of the amazon coast: Evidence for localized sources in contrast to massive regional biomass burning. Environmental Pollution, 268, p.115958. https://doi.org/10.1016/j.envpol.2020.115958.

Ranjbar, M. H., Hadjizadeh Zaker, N. (2018). Numerical modeling of general circulation, thermohaline structure, and residence time in Gorgan Bay, Iran. Ocean Dynamics, 68(1), pp.35-46. https://doi.org/10.1007/s10236-017-1116-6.

Ranjbar, M. H., Alaee, M. J., Nazarali, M. (2019). A modeling study of the impact of increasing water exchange rate on water quality of a semi-enclosed bay. Ecological Engineering, 136, pp.177-184. https://doi.org/10.1016/j.ecoleng.2019.05.024.

Ranjbar Jafarabadi, A., Mashjoor, S., Mohamadjafari Dehkordi, S., Riyahi Bakhtiari, A., Cappello, T. (2020). Steroid fingerprint analysis of endangered Caspian seal (Pusa caspica) through the Gorgan Bay (Caspian Sea). Environmental Science & Technology, 54(12), pp.7339-7353. https://doi.org/10.1021/acs.est.0c01479.

Sadeghi Pasvisheh, R., Eurie Forio, M. A., Ho, L. T., Goethals, P. L. (2021). Evidence-Based Management of the Anzali Wetland System (Northern Iran) Based on Innovative Monitoring and Modeling Methods. Sustainability, 13(10), p.5503. https://doi.org/10.3390/su13105503.

Sheikh Fakhradini, S., Moore, F., Keshavarzi, B., Lahijanzadeh, A. (2019). Polycyclic aromatic hydrocarbons (PAHs) in water and sediment of Hoor Al-Azim wetland, Iran: a focus on source apportionment, environmental risk assessment, and sediment-water partitioning. Environmental monitoring and assessment, 191(4), pp.1-18. https://doi.org/10.1007/s10661-019-7360-0.

Sinkakarimi, M. H., Binkowski, L. J., Hassanpour, M., Rajaei, G., Ahmadpour, M., Levengood, J. M. (2018). Metal concentrations in tissues of Gadwall and common teal from Miankaleh and Gomishan international wetlands, Iran. Biological trace element research, 185(1), pp.177-184. https://doi.org/10.1007/s12011-017-1237-2.

Taheri Azad, L., Esmaili Sari, A., Rezai Tavabe, K. (2009). Determination of rest-oil pollution (polycyclic aromatic hydrocarbons) in surface water of three international wetlands of Iran. J. Environ. Res. Develop, 4, pp.310-320.

Tenkouano, G. T., Cumming, B. F., Jamieson, H. E. (2019). Geochemical and ecological changes within Moira Lake (Ontario, Canada): A legacy of industrial contamination and remediation. Environmental Pollution, 247, pp.980-988. https://doi.org/10.1016/j.envpol.2019.01.019.

Thuy, H.T.T., Loan, T.T.C., Luu, P.T., Van Dong, N., Bao, L.D., Phuong, T.H., Khanh, N.T., Yen, T.T.H. Huy, D.X. (2021). Spatial and temporal variations of PAHs in surface sediments of estuarine and coast of CanGio wetland, Vietnam. Environmental Science and Pollution Research, 28(10), pp.11962-11975. https://doi.org/10.1007/s11356-020-08523-8.

Townsend, K. R., Lu, H. C., Sharley, D. J., Pettigrove, V. (2019). Associations between microplastic pollution and land use in urban wetland sediments. Environmental Science and Pollution Research, 26(22), pp.22551-22561. https://doi.org/10.1007/s11356-019-04885-w.

United States Environmental Protection Agency (USEPA), 2015. National recommended water quality criteria. https://www.epa.gov/wqc/national-recommended-water-quality-criteria-human-health-criteria-table.

Wang, Z., Liu, S., Zhang, T. (2019). Characteristics of polycyclic aromatic hydrocarbons (PAHs) in soil horizon from high-altitude mountains in Northeastern China. Chemosphere, 225, pp.93-103. https://doi.org/10.1016/j.chemosphere.2019.03.001.

Wang, N., Wang, J., Li, Y., Xing, M., Zhou, B., Li, X., Li, X., Kong, W., Ding, L. Liu, H. (2020). Occurrences, Retention and Risk Assessments of PAHs in Beidagang Wetland in Tianjin, China. Bulletin of Environmental Contamination and Toxicology, 105(4), pp.607-612. https://doi.org/10.1007/s00128-020-02997-5.

Wang, C., Ma, L., Zhang, Y., Chen, N., Wang, W. (2022). Spatiotemporal dynamics of wetlands and their driving factors based on PLS-SEM: A case study in Wuhan. Science of The Total Environment, 806, p.151310. https://doi.org/10.1016/j.scitotenv.2021.151310.

Wang, C., Zou, X., Gao, J., Zhao, Y., Yu, W., Li, Y., Song, Q. (2016). Pollution status of polycyclic aromatic hydrocarbons in surface sediments from the Yangtze River Estuary and its adjacent coastal zone. Chemosphere, 162, pp.80-90. https://doi.org/10.1016/j.chemosphere.2016.07.075.

World Photography Organisation, 2022. Painful Death of Birds. https://www.worldphoto.org/sony-world-photography-awards/winners-galleries/2022/professional/painful-death-birds-mehdi-mohebi

Xiu, L., Yan, C., Li, X., Qian, D., Feng, K. (2019). Changes in wetlands and surrounding land cover in a desert area under the influences of human and climatic factors: A case study of the Hongjian Nur region. Ecological indicators, 101, pp.261-273. https://doi.org/10.1016/j.ecolind.2019.01.025.

Xu, T., Weng, B., Yan, D., Wang, K., Li, X., Bi, W., Li, M., Cheng, X. Liu, Y. (2019). Wetlands of international importance: Status, threats, and future protection. International journal of environmental research and public health, 16(10), p.1818. https://doi.org/10.3390/ijerph16101818.

Xu, Y., Liu, T., Zhu, X., Ji, G. (2019). Quantitative analysis of genetic associations in the biodegradative pathway of PAHs in wetland sediments of the Bohai coast region. Chemosphere, 218, pp.282-291. https://doi.org/10.1016/j.chemosphere.2018.11.059.

Yancheshmeh, R. A., Bakhtiari, A. R., Mortazavi, S., Savabieasfahani, M. (2014). Sediment PAH: contrasting levels in the Caspian Sea and Anzali Wetland. Marine Pollution Bulletin, 84(1-2), pp.391-400. https://doi.org/10.1016/j.marpolbul.2014.05.001.

Yang, W., Wang, Z., Hua, P., Zhang, J., Krebs, P. (2021). Impact of green infrastructure on the mitigation of road-deposited sediment induced stormwater pollution. Science of the Total Environment, 770, p.145294. https://doi.org/10.1016/j.scitotenv.2021.145294.

Yang, J., Yang, Y., Chen, R. S., Meng, X. Z., Xu, J., Qadeer, A., Liu, M. (2018). Modeling and evaluating spatial variation of polycyclic aromatic hydrocarbons in urban lake surface sediments in Shanghai. Environmental Pollution, 235, pp.1-10. https://doi.org/10.1016/j.envpol.2017.12.032.

Zafarani, G. G., Karbalaei, S., Golshani, R., Pustokhina, I., Walker, T. R. (2022). Baseline occurrence, distribution and sources of PAHs, TPH, and OCPs in surface sediments in Gorgan Bay, Iran. Marine Pollution Bulletin, 175, p.113346. https://doi.org/10.1016/j.marpolbul.2022.113346.

Zhang, Y., Cheng, D., Lei, Y., Song, J., Xia, J. (2022). Spatiotemporal distribution of polycyclic aromatic hydrocarbons in sediments of a typical river located in the Loess Plateau, China: Influence of human activities and land-use changes. Journal of Hazardous Materials, 424, p.127744. https://doi.org/10.1016/j.jhazmat.2021.127744.

Zhao, Z., Gong, X., Zhang, L., Jin, M., Cai, Y., Wang, X. (2021 a). Riverine transport and water-sediment exchange of polycyclic aromatic hydrocarbons (PAHs) along the middle-lower Yangtze River, China. Journal of Hazardous Materials, 403, p.123973. https://doi.org/10.1016/j.jhazmat.2020.123973.

Zhao, C., Xu, J., Shang, D., Zhang, Y., Zhang, J., Xie, H., Kong, Q. Wang, Q. (2021 b). Application of constructed wetlands in the PAH remediation of surface water: A review. Science of The Total Environment, 780, p.146605. https://doi.org/10.1016/j.scitotenv.2021.146605.

Zhang, Y., Cui, B., Zhang, Q., Liu, X. (2015). Polycyclic aromatic hydrocarbons in the food web of coastal wetlands: distribution, sources and potential toxicity. Clean–Soil, Air, Water, 43(6), pp.881-891. https://doi.org/10.1002/clen.201400305.

Zhang, J., Li, R., Zhang, X., Bai, Y., Cao, P., Hua, P. (2019). Vehicular contribution of PAHs in size dependent road dust: a source apportionment by PCA-MLR, PMF, and Unmix receptor models. Science of The Total Environment, 649, pp.1314-1322. https://doi.org/10.1016/j.scitotenv.2018.08.410.

Zhang, R., Han, M., Yu, K., Kang, Y., Wang, Y., Huang, X., Li, J. Yang, Y. (2021). Distribution, fate and sources of polycyclic aromatic hydrocarbons (PAHs) in atmosphere and surface water of multiple coral reef regions from the South China Sea: A case study in spring-summer. Journal of Hazardous Materials, 412, p.125214. https://doi.org/10.1016/j.jhazmat.2021.125214.

Zuloaga, O., Prieto, A., Ahmed, K., Sarkar, S.K., Bhattacharya, A., Chatterjee, M., Bhattacharya, B.D. Satpathy, K.K. (2013). Distribution of polycyclic aromatic hydrocarbons in recent sediments of Sundarban mangrove wetland of India and Bangladesh: a comparative approach. Environmental earth sciences, 68(2), pp.355-367. https://doi.org/10.1007/s12665-012-1743-7.

Supplementary Information

Occurrence and source of PAHs in Miankaleh International Wetland in Iran

Mahsa Rokhbar [a], Behnam Keshavarzi [a,*], Farid Moore [a], Mehdi Zarei [a], Peter S. Hooda [b], Michael J.Risk [c]

[a] Department of Earth Sciences, College of Science, Shiraz University, 71454 Shiraz, Iran.

[b] Department of Geography, Geology and the Environment, Kingston University London, Kingston Upon Thames KT12EE, UK.

[C] Department of Earth Sciences, McMaster University, Hamilton, Ontario, L8S 4M1, Canada.

[*] Corresponding author.

E-mail addresses: BKeshavarzi@shirazu.ac.ir (B. Keshavarzi)

Table S1. Physio-chemical parameters of water in Miankaleh Wetland

Parameter	Min.	Max.	Mean	Med.	S.D.
EC (mS/Cm)	0.80	23.40	16.00	20.80	8.60
pH	7.20	28.30	10.20	8.40	5.70
Eh (mV)	-17.90	173.00	94.80	90.20	55.40
T (ºC)	24.80	31.60	27.70	27.90	2.10
DO* (mg/L)	4.40	16.00	9.60	8.70	3.00

* Dissolved Oxygen

Table S2. Physio-chemical parameters of sediment in Miankaleh Wetland

Parameter	Min.	Max.	Mean	Med.	S.D.
EC (mS/cm)	1.00	65.60	10.60	8.50	11.20
CEC (meq/100g)	3.90	112.20	39.40	31.50	25.40
Sand %	0.00	88.60	41.90	36.70	27.10
Silt %	2.00	63.10	26.90	26.00	15.50
Clay %	8.20	57.30	31.20	31.80	14.90
***Organic Matter %**	2.00	16.30	8.30	7.50	3.90
$CaCO_3$ %	1.70	35.10	14.10	14.10	7.30
pH	6.80	9.50	8.10	8.10	0.70

* Determined as loss-on-ignition

Table S3. The list of PAHs and their abbreviations

PAHs	Abbreviations	Aromatic Rings
Naphthalene	Nap	2
Acenaphthylene	Acy	3
Acenaphthene	Ace	3
Fluorene	Flu	3
Phenanthrene	Phe	3
Anthracene	Ant	3
Fluoranthene	Fl	4
Pyrene	Pyr	4
Benz(a)anthracene	BaA	4
Chrysene	Chr	4
Benzo(b)fluoranthene	BbF	5
Benzo(k)fluoranthene	BkF	5
Benzo(a)pyrene	BaP	5
Indeno(1,2,3-C,D)pyrene	InP	6
Dibenz(a,h)anthracene	DahA	5
Benzo(g,h,i)perylene	BghiP	6

Table S4. Spearman's correlation coefficient between the concentration of PAHs in water samples and water parameters in Miankaleh wetland

	∑ PAHs (ng/L)	**EC (mS/Cm)**	**pH**	**Eh (mV)**	**T (°C)**	**DO (mg/L)**
∑ PAHs (ng/L)	1.00					
EC (mS/Cm)	0.31	1.00				
pH	-.620*	-0.18	1.00			
Eh (mV)	-0.04	0.18	-0.43	1.00		
T	-0.19	-0.22	0.02	0.20	1.00	
DO (mg/L)	0.02	-0.45	0.16	-0.38	0.48	1.00

* Correlation is significant at the 0.05 level (2-tailed).

Table S5. Spearman's correlation coefficient between the concentration of PAHs in sediment samples and sediment parameters in Miankaleh Wetland

	∑PAHs (µg/kg dw)	EC (mS /cm)	CEC (meq/100g)	Sand %	Silt %	Clay %	Organic Matter %	$CaCO_3$ %
∑PAHs (µg/kg dw)	1.00							
EC (mS /cm)	-0.14	1.00						
CEC (meq/100g)	0.31	0.35	1.00					
Sand %	-0.11	-.42*	-.59**	1.00				
Silt %	0.08	0.31	.43*	-.92**	1.00			
Clay %	0.21	.42*	.69**	-.88**	.67**	1.00		
Organic Matter %	0.10	.68**	.65**	-.75**	.60**	.82**	1.00	
$CaCO_3$ %	-0.25	-0.09	-.36*	.49**	-.52**	-0.26	-0.15	1.00

* Correlation is significant at the 0.05 level (2-tailed).

** Correlation is significant at the 0.01 level (2-tailed).

Table S6. The Quantization error (QE) and Topographical error (TE) were computed at different map sizes

Map Size	QE	TE
(5 × 5)	7.40	0.00
(2 × 13)	5.83	0.00
(13 × 2)	5.99	0.23
(3 × 9)	6.29	0.00
(9 × 3)	5.13	0.00
(4 × 7)	6.10	0.00
(7 × 4)	6.26	0.00
(14 × 2)	4.95	0.00
(2 × 14)	4.66	0.00
(5 × 6)	6.45	0.00
(6 × 5)	5.70	0.00
(2 × 15)	4.43	0.00
(15 × 2)	4.44	0.00
(10 × 3)	4.97	0.00
(3 × 10)	5.21	0.00
(16 × 2)	4.37	0.00
(2 × 16)	3.55	0.00
(4 × 8)	5.82	0.00
(8 × 4)	4.75	0.00
(11 × 3)	4.28	0.08

(3 × 11)	5.31	0.00
(2 × 17)	3.41	0.00
(17 × 2)	**2.85**	**0.00**
(7 × 5)	5.05	0.00
(5 × 7)	5.30	0.00